Journal of the Egyptian Mathematical Society (2016) **24**, 138–142

Egyptian Mathematical Society

Journal of the Egyptian Mathematical Society

www.etms-eg.org
www.elsevier.com/locate/joems

ORIGINAL ARTICLE

Rheological properties of Reiner-Rivlin fluid model for blood flow through tapered artery with stenosis

Noreen Sher Akbar [a,*], **S. Nadeem** [b], **Kh.S. Mekheimer** [c]

[a] *DBS&H, CEME, National University of Sciences and Technology, Islamabad, Pakistan*
[b] *Department of Mathematics, Quaid-i-Azam University, 45320 Islamabad 44000, Pakistan*
[c] *Mathematics Department, Faculty of Science, Al-Azhar University, Nasr City, 11884 Cairo, Egypt*

Received 20 December 2013; revised 23 October 2014; accepted 25 October 2014
Available online 11 February 2015

KEYWORDS

Reiner-Rivlin fluid;
Blood flow;
Tapered artery;
Stenosis;
Perturbation solution

Abstract In the present article, we have analyzed the Reiner-Rivlin fluid model for blood flow through a tapered artery with a stenosis. The constitutive equations for a Reiner-Rivlin fluid have been modeled in cylindrical coordinates. A perturbation series in dimensionless Reiner-Rivlin fluid parameter ($\lambda_1 \ll 1$) have been used to obtain explicit forms for the velocity, resistance impedance, wall shear stress and shearing stress at the stenosis throat. The graphical results of different type of tapered arteries (i.e converging tapering, diverging tapering, non-tapered artery) have been examined for different parameters of interest.

2010 MATHEMATICS SUBJECT CLASSIFICATION: 76Zxx; 76Mxx; 92C10

1. Introduction

In the arterial systems of humans or animals, it is quite common to find localized narrowings, commonly called stenosis, caused by intravascular plaques. These stenosis disturb the normal pattern of blood flow through the artery [1]. Pulsatile flow of blood through a stenosed porous medium under the influence of body acceleration has been studied by El-Shahed [2]. He mentioned that the investigations of blood flow through arteries are of considerable importance in many cardiovascular diseases particularly atherosclerosis. The effects of pulsatility, stenosis and non-Newtonian behavior of blood, assuming the blood to be represented by Herschel–Bulkley fluid, are simultaneously considered by Sankara and Hemalatha [3]. Among the various arterial diseases the development of arteriosclerosis in blood vessels is quite common which may be attributed to accumulation of lipids in the arterial wall or pathological changes in the tissue structure [4].

The mathematical modeling of non-Newtonian nature of blood flow through a stenosed tube has been studied by Shukla et al. [5,6] and Chaturani and Ponnalagar Samy [7]. Blood flow in a stenosed tube has been modeled for couple stress fluid by Pralhad and Schultz [8]. Hall [9] and Porenta et al. [10] pointed out that most of the vessels could be considered as long and narrow, slowly tapering cones. Thus the effects of vessel

* Corresponding author.
E-mail address: noreensher1@gmail.com (N.S. Akbar).
Peer review under responsibility of Egyptian Mathematical Society.

ELSEVIER Production and hosting by Elsevier

http://dx.doi.org/10.1016/j.joems.2014.10.007
1110-256X

tapering together with the non-Newtonian behavior of the streaming blood seem to be equally important and hence certainly deserve special attention [11,12]. Some recent studies which have been made to study the blood flow properties are cited in the refs. [13–20].

With the above motivation, an attempt is made in the present investigation to develop a mathematical model in order to study the characteristics of the Reiner Rivlin fluid model for blood flow through a tapered arteries in the presence of stenosis. The governing equations are solved analytically by regular perturbation method. The expression for velocity, resistance impedance, wall shear stress and shearing stress at the stenosis throat has been calculated. At the end, the physical features of various emerging parameters have been discussed by plotting the graphs. Trapping phenomena have been discussed at the end of the article.

2. Mathematical formulation

Let us consider an incompressible flow of Reiner Rivlin fluid having constant viscosity μ and density ρ in a tube having length L. We are considering cylindrical coordinate system (r, θ, z) such that $\bar{u}$ and $\bar{w}$ are the velocity component in $\bar{r}$ and $\bar{z}$ direction respectively. Further we assume that $r = 0$ is taken as the axis of the symmetry of the tube. The geometry of the stenosis which is assumed to be symmetric can be described as [11]

$$h(z) = d(z)[1 - \eta_1(b^{n-1}(z-a) - (z-a)^n)], \quad a \leqslant z \leqslant a+b, \tag{1}$$

$$= d(z), \quad \text{otherwise} \quad d(z) = d_0 + \xi z, \tag{2}$$

where $d(z)$ is the radius of the tapered arterial segment in the stenotic region, d_0 is the radius of the non-tapered artery in the non-stenoic region, ξ is the tapering parameter, b is the length of stenosis, $(n \geqslant 2)$ is a parameter determining the shape of the constriction profile and referred to as the shape parameter (the symmetric stenosis occurs for $n = 2$) and a indicates its location as shown in Fig. 1. The parameter η is defined as

$$\eta = \frac{\delta^* n^{\frac{n}{n-1}}}{d_0 b^n (n-1)}, \tag{3}$$

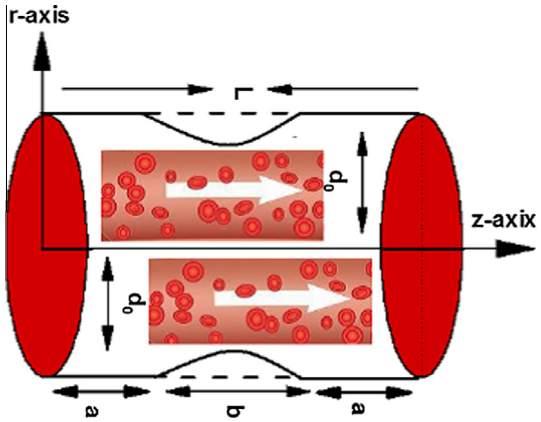

Figure 1 Geometry of an axially nonsymmetrical stenosis in the artery.

The equations governing the steady incompressible Reiner-Rivlin fluid are given as

$$\frac{\partial \bar{u}}{\partial \bar{r}} + \frac{\bar{u}}{\bar{r}} + \frac{\partial \bar{w}}{\partial \bar{z}} = 0, \tag{4}$$

$$\rho\left(\bar{u}\frac{\partial}{\partial \bar{r}} + \bar{w}\frac{\partial}{\partial \bar{z}}\right)\bar{u} = -\frac{\partial \bar{p}}{\partial \bar{r}} + \frac{1}{\bar{r}}\frac{\partial}{\partial \bar{r}}(\bar{r}\bar{\tau}_{\bar{r}\bar{r}}) + \frac{\partial}{\partial \bar{z}}(\bar{\tau}_{\bar{r}\bar{z}}) - \frac{\bar{\tau}_{\bar{\theta}\bar{\theta}}}{\bar{r}}, \tag{5}$$

$$\rho\left(\bar{u}\frac{\partial}{\partial \bar{r}} + \bar{w}\frac{\partial}{\partial \bar{z}}\right)\bar{w} = -\frac{\partial \bar{p}}{\partial \bar{z}} + \frac{1}{\bar{r}}\frac{\partial}{\partial \bar{r}}(\bar{r}\bar{\tau}_{\bar{r}\bar{z}}) + \frac{\partial}{\partial \bar{z}}(\bar{\tau}_{\bar{z}\bar{z}}). \tag{6}$$

The Cauchy stress $\bar{\tau}_{ij}$ for a Reiner Rivlin fluid is given by [12]

$$\bar{\tau}_{ij} = -\bar{p}\delta_{ij} + \mu e_{ij} + \mu_c e_{ik} e_{kj}, \quad i,j = \bar{r}, \bar{z}, \bar{\theta}, \tag{7}$$

where $\bar{\tau}_{ij}$ is the stress tensor, e_{ij} is the rate of strain tensor, δ_{ij} is the Kronecker delta, μ is the coefficient of viscosity and μ_c is the coefficient of cross viscosity.

We introduce the non-dimensional variables

$$r = \frac{\bar{r}}{d_0},\ z = \frac{\bar{z}}{b},\ w = \frac{\bar{w}}{u_0},\ u = \frac{b\bar{u}}{u_0\delta},\ p = \frac{d_0^2\bar{p}}{u_0 b\mu},\ h = \frac{\bar{h}}{d_0},$$
$$\mathrm{Re} = \frac{\rho b u_0}{\mu},\ \tilde{\tau}_{rr} = \frac{b\bar{\tau}_{rr}}{u_0\mu},\ \tilde{\tau}_{rz} = \frac{d_0\bar{\tau}_{rz}}{u_0\mu},\ \tilde{\tau}_{zz} = \frac{b\bar{\tau}_{zz}}{u_0\mu},\ \tilde{\tau}_{\theta\theta} = \frac{b\bar{\tau}_{\theta\theta}}{u_0\mu},$$
$$\lambda_1 = \frac{\mu_c u_0}{\mu b}, \tag{8}$$

where u_0 is the velocity averaged over the section of the tube of the width d_0.

Making use of Eqs. (7) and (8), Eqs. (4)–(6), the appropriate equations describing the steady flow of an incompressible Reiner Rivlin fluid in the case of mild stenosis $\left(\frac{\delta^*}{d_0} \ll 1\right)$, subject to the additional conditions [11] i.e

$$(i)\ \frac{\mathrm{Re}\delta^* n^{\left(\frac{1}{n-1}\right)}}{b} \ll 1, \quad (ii)\ \frac{d_0 n^{\left(\frac{1}{n-1}\right)}}{b} \sim O(1), \tag{9}$$

can be written as

$$\frac{\partial u}{\partial r} + \frac{u}{r} + \frac{\partial w}{\partial z} = 0, \tag{10}$$

$$\frac{\partial p}{\partial r} = 0, \tag{11}$$

$$\frac{\partial p}{\partial z} = \frac{1}{r}\frac{\partial}{\partial r}\left[r\left(\left(\frac{\partial w}{\partial r}\right) + \lambda_1\left(2\frac{\partial w}{\partial r}\frac{\partial w}{\partial z}\right)\right)\right]. \tag{12}$$

The corresponding boundary conditions are

$$\frac{\partial w}{\partial r} = 0 \quad \text{at } r = 0,\ w = 0 \quad \text{at } r = h(z), \tag{13}$$

where

$$h(z) = (1 + \xi z)[1 - \eta_1((z-\sigma) - (z-\sigma)^n)], \quad \sigma \leqslant z \leqslant \sigma + 1, \tag{14}$$

and

$$\eta_1 = \frac{\delta n^{\frac{n}{n-1}}}{(n-1)},\ \delta = \frac{\delta^*}{d_0},\ \sigma = \frac{a}{b},\ \xi' = \frac{\xi b}{d_0} \tag{15}$$

in which $(\xi = \tan\phi)$, ϕ is called tapered angle and for converging tapering $(\phi < 0)$, non-tapered artery $(\phi = 0)$ and the diverging tapering $(\phi > 0)$.

3. Solution of the problem

Since Eq. (12) is non-linear equation. Therefore, we are seeking the perturbation solutions, for perturbation solution, we expand w, Q and p by taking λ_1 as perturbation parameter. The solutions for velocity and pressure gradient, satisfying boundary conditions take the form

$$w = \left(\frac{r^2-h^2}{4}\right)\frac{dp}{dz} + \lambda_1\left(\frac{dp}{dz}\frac{dp'}{dz}\frac{1}{16}((r^4-h^4)-2h^2(r^2-h^2)) + \left(\frac{dp}{dz}\right)^2\frac{hh'}{4}(r^2-h^2)\right), \tag{16}$$

$$\frac{dp}{dz} = -\frac{16Q}{h^4} + \lambda_1\left(\frac{8Q}{3h^2}\left(-\frac{16Q}{h^4}\right)' - \frac{256Q^2h'}{h^7}\right), \tag{17}$$

The pressure drop ($\Delta p = p$ at $z = 0$ and $\Delta p = -p$ at $z = L$) across the stenosis between the section $z = 0$ and $z = L$ is obtain from (19) as done by [11]

$$\Delta p = \int_0^L \left(-\frac{dp}{dz}\right)dz. \tag{18}$$

3.1. Resistance impedance

The resistance impedance is obtain from Eq. (18) as

$$\tilde{\lambda} = \frac{\Delta p}{Q} = \left\{\int_0^a F(z)\Big|_{h=1}dz + \int_a^{a+b} F(z)dz + \int_{a+b}^L F(z)\Big|_{h=1}dz\right\}, \tag{19}$$

where

$$F(z) = \frac{16}{h^4} + \lambda_1\left(-\frac{8}{3h^2}\left(-\frac{16Q}{h^4}\right)' + \frac{256Qh'}{h^7}\right),$$

3.2. Expression for the wall shear stress

The nonzero dimensionless shear stress is given by

$$\tilde{\tau}_{rz} = \left(2\left(\frac{\partial w}{\partial r}\right) + \lambda_1\left(2\frac{\partial w}{\partial r}\frac{\partial w}{\partial z}\right)\right)\Big|_{r=h}, \tag{20}$$

So

$$\tilde{\tau}_{rz} = a_1r^7 + a_2r^5 + a_3r^3 + a_4r + a_5, \tag{21}$$

The expression for shearing stress at the stenosis throat i.e. the wall shear at the maximum height of the stenosis located at $z = \frac{a}{b} + \frac{1}{n^{\frac{n}{n-1}}}$ i.e $\tilde{\tau}_s = \tilde{\tau}_{rz}|_{h=1-\delta}$ is

$$\tilde{\tau}_s = a_1r^7 + a_2r^5 + a_3r^3 + a_4r + a_5\big|_{h=1-\delta}. \tag{22}$$

The final expression for the dimensionless resistance to λ, wall shear stress τ_{rz} and the shearing stress at the throat τ_s by

$$\lambda = \frac{1}{3}\left\{\left(1-\frac{b}{L}\right)\left(16 + \lambda_1\left(-\frac{8}{3}(-16Q)' + 256Qh'\right)\right) + \frac{1}{L}\int_a^{a+b} F(z)dz\right\}, \tag{23}$$

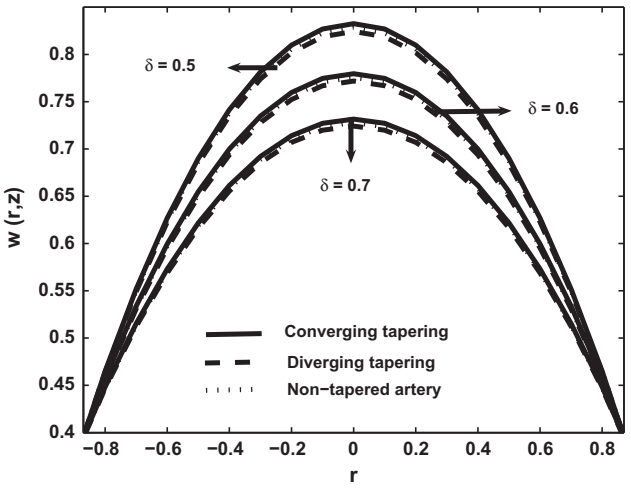

Figure 2 Variation of velocity profile for $Q = 0.3, \sigma = 0.0$, $z = 0.5, n = 2, \lambda_1 = 0.3$.

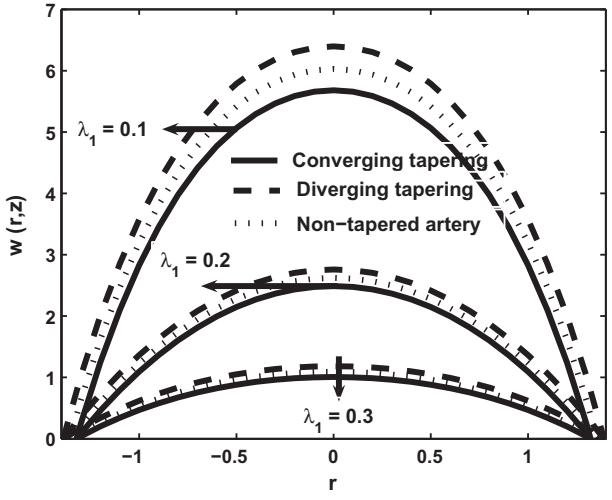

Figure 3 Variation of velocity profile for $Q = 0.3, \sigma = 0.0$, $z = 0.3, n = 2, \delta = 0.3$.

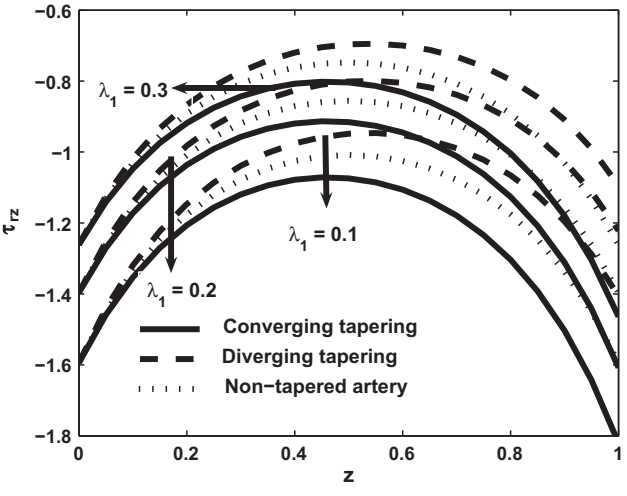

Figure 4 Variation of wall shear stress for $Q = 0.3, n = 2$, $\sigma = 0.0, \delta = 0.3$.

$$\tau_{rz} = \frac{1}{4Q}\left(a_1 r^7 + a_2 r^5 + a_3 r^3 + a_4 r + a_5,\right), \tag{24}$$

$$\tau_s = \frac{1}{4Q}\left(a_1 r^7 + a_2 r^5 + a_3 r^3 + a_4 r + a_5,\big|_{h=1-\delta}\right), \tag{25}$$

where

$$\lambda = \frac{\tilde{\lambda}}{\lambda_0},\ \tau_{rz} = \frac{\tilde{\tau}_{rz}}{\tau_0},\ \tau_s = \frac{\tilde{\tau}_s}{\tau_0},\ \lambda_0 = 3L,\ \tau_0 = 4Q,$$

and λ_0, τ_0 are the resistance to flow and the wall shear stress for a flow in a normal artery (no stenosis). Where a_1 to a_5 are obtained using Mathematica.

4. Numerical results and discussion

The quantitative effects of the Reiner Rivlin fluid parameter λ_1, the stenosis shape n and maximum height of the stenosis δ for converging tapering, diverging tapering and non-tapered arteries for Reiner Rivlin fluid Figs. 2–8 are prepared. The variation of axial velocity for λ_1, n, and δ for the case of a converging tapering, diverging tapering and non-tapered arteries are displayed in Figs. 2 and 3. In Figs. 2 and 3 we observed

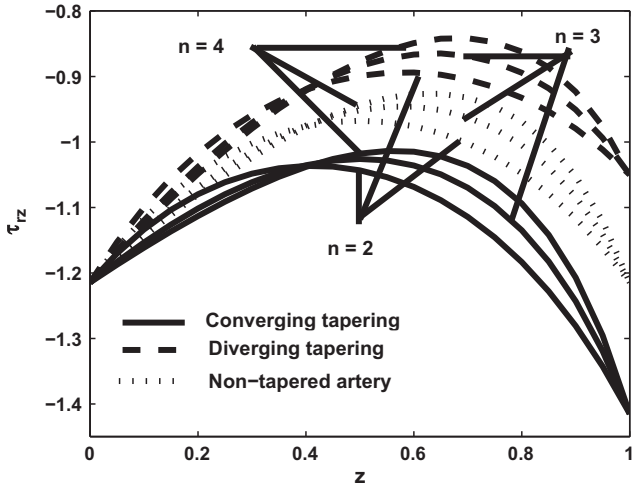

Figure 5 Variation of wall shear stress for $Q = 0.3, \lambda_1 = 0.2, \sigma = 0.0, \delta = 0.3$.

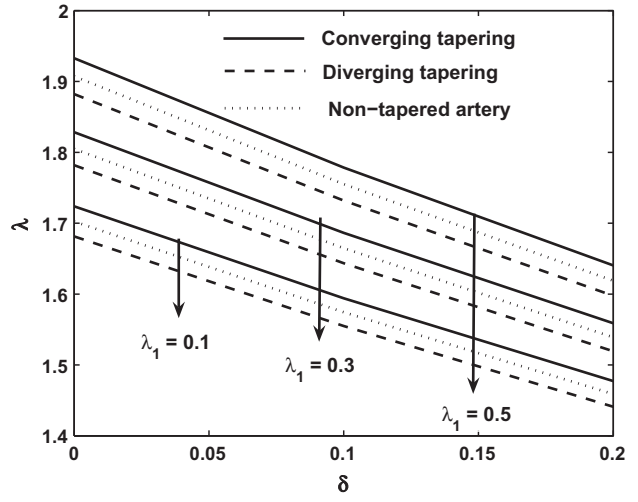

Figure 6 Variation of resistance for $Q = 0.3, L = 1, \sigma = 0.0, b = 0.6, n = 2, z = 0.5$.

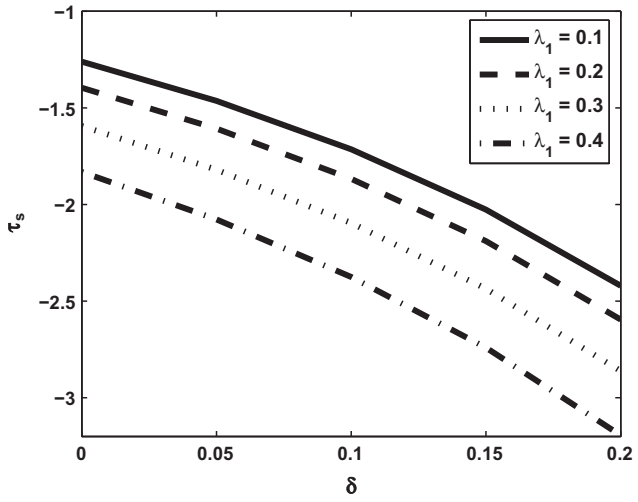

Figure 7 Variation of shear stress at the stenosis throat for $Q = 0.3$.

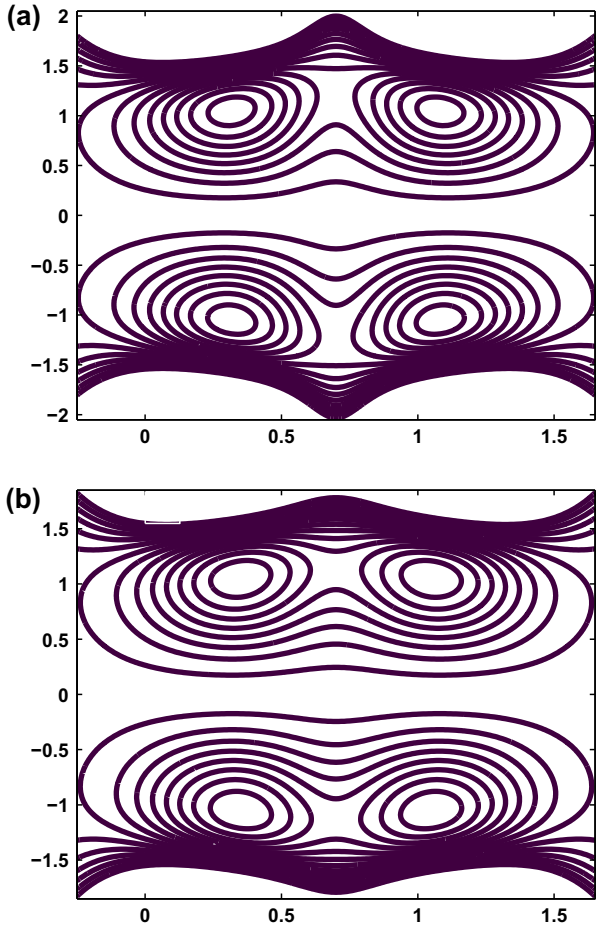

Figure 8 Stream lines for different values of λ_1: (a) $\lambda_1 = 0.1$, (b) $\lambda_1 = 0.3$ other parameters are $Q = 0.3, \delta = 0.1, n = 2$.

that with an increase in λ_1 and δ velocity profile decreases. It is also seen that for the case of converging tapering velocity gives larger values as compared to the case of diverging tapering and non-tapered arteries. Figs. 4 and 5 show how the converging tapering, diverging tapering and non-tapered arteries influence on the wall shear stress τ_{rz}. It is observed that with an increase in λ_1 and n shear stress increases, the stress yield diverging tapering with tapered angle $\phi > 0$, converging tapering with tapered angle $\phi < 0$ and non-tapered artery with tapered angle $\phi = 0$. In Fig. 6 we notice that the impedance resistance increases for converging tapering, diverging tapering and non-tapered arteries when we increase λ_1. We also observed that resistive impedance in a diverging tapering appear to be smaller than those in converging tapering because the flow rate is higher in the former than that in the latter, as anticipated and impedance resistance attains its maximum values in the symmetric stenosis case ($n = 2$). Finally, Fig. 7 is prepared to see the variation of the shearing stress at the stenosis throat τ_s with δ. It is analyzed through figures that shearing stress at the stenosis throat decreases with an increase in λ_1. Fig. 8 shows the stream lines for different values of λ_1. It is depicted that the size of the trapping bolus increases with an increase in Reiner Rivlin fluid parameter, while decreases with an increase in the height of the stenosis shape.

Acknowledgments

Authors are very thankful to the reviewers for very useful suggestions to improve the manuscript.

References

[1] J. Mazumnardar, An Introduction to Mathematical Physiology and Biology, Australian Mathematical Society, 1989.
[2] M. El-Shahed, Pulsatile flow of blood through a stenosed porous medium under periodic body acceleration, Appl. Math. Comput. 138 (2003) 479–488.
[3] D.S. Sankara, K. Hemalatha, Pulsatile flow of Herschel–Bulkley fluid through stenosed arteries—a mathematical model, Int. J. Non-Linear Mech. 41 (2006) 979–990.
[4] D. Liepsch, M. Singh, L. Martin, Experimental analysis of the influence of stenotic geometry on steady flow, Biorheology 29 (1992) 419–431.
[5] J.B. Shukla, R.S. Parihar, B.R.P. Rao, Effects of stenosis on non-Newtonian flow of blood in an artery, Bull. Math. Biol. 42 (1980) 283–294.
[6] J.B. Shukla, R.S. Parihar, S.P. Gupta, Biorheological aspects of blood flow through artery with mild stenosis: effects of peripheral layer, Biorheology 17 (1980) 403–410.
[7] P. Chaturani, R. Ponnalagar Samy, A study of non-Newtonian aspects of blood flow through stenosed arteries and its applications in arterial diseases, Biorheology 22 (1985) 521–531.
[8] R.N. Pralhad, D.H. Schultz, Modeling of arterial stenosis and its applications to blood diseases, Math. Biosci. 190 (2004) 203–220.
[9] P. Hall, Unsteady viscous flow in a pipe of slowly varying cross-section, J. Fluid Mech. 64 (1974) 209–226.
[10] G. Porenta, G.F. Young, T.R. Rogge, A finite element model of blood flow in arteries including taper, branches and obstructions, J. Biomech. Eng. 108 (1986) 161–167.
[11] Kh. S. Mekheimer, M.A. El Kot, The micropolar fluid model for blood flow through a tapered artery with a stenosis, Acta Mech. Sin. 24 (2008) 637–644.
[12] S. Panja, P.R. Sengupta, Hydromagnetic flow of Reiner-Rivlin fluid between two coaxial circular cylinders with porous walls, Comput. Math. Appl. 32 (1996) 1–4.
[13] Noreen Sher Akbar, Heat and mass transfer effects on Careau fluid model for blood flow through tapered arteries with stenosis, Int. J. Bio Math. 7 (2014) 1450004.
[14] Noreen Sher Akbar, MHD peristaltic flow with carbon nanotubes in an asymmetric channel, J. Comput. Theor. Nanosci. 11 (2014) 1323–1329.
[15] Noreen Sher Akbar, S. Nadeem, Simulation of peristaltic flow of chyme in small intestine for couple stress fluid, Meccanica 49 (2014) 325–334.
[16] Noreen Sher Akbar, Metallic nanoparticles analysis for the peristaltic flow in an asymmetric channel with MHD, IEEE Trans. Nanotechnol. 13 (2014) 357–361.
[17] Noreen Sher Akbar, Peristaltic flow with Maxwell carbon nanotubes Suspensions, J. Comput. Theor. Nanosci. 11 (7) (2014) 1642–1648.
[18] Noreen Sher Akbar, Endoscopic effects on the Peristaltic flow of Cu-water nanofluid, J. Comput. Theor. Nanosci. 11 (6) (2014) 1150–1155.
[19] Noreen Sher Akbar, MHD Eyring Prandtl fluid flow with convective boundary conditions in small intestines, Int. J. Bio Math. 6 (2013) 350034.
[20] Noreen Sher Akbar, Double-diffusive natural convective peristaltic flow of a Jeffrey nanofluid in a porous channel, Heat Transfer Res. 45 (4) (2014) 293–307.